SCIENCE CHINA
Information Sciences

• RESEARCH PAPER •

June 2024, Vol. 67, Iss. 6, 162206:1–162206:14
https://doi.org/10.1007/s11432-023-4038-3

Accumulated-state-error-based event-triggered sampling scheme and its application to H_∞ control of sampled-data systems

Xian-Ming ZHANG[1], Qing-Long HAN[1*], Bao-Lin ZHANG[2], Xiaohua GE[1] & Dawei ZHANG[3]

[1]*School of Science, Computing, and Engineering Technologies, Swinburne University of Technology, Melbourne* VIC 3122*, Australia;*
[2]*College of Automation and Electronic Engineering, Qingdao University of Science & Technology, Qingdao* 266061*, China;*
[3]*School of Mathematics, Shandong University, Jinan* 250100*, China*

Received 10 December 2023/Revised 8 February 2024/Accepted 14 May 2024/Published online 28 May 2024

Abstract This paper is concerned with event-triggered H_∞ control of sampled-data systems. Its novelties lie in three aspects: (i) A novel accumulated-state-error-based event-triggered scheme is introduced by comparing the integral of the state error from t_k to t with the system state sampled at t_k. This condition works well due to the fact that the so-called Zeno behaviour does not occur. (ii) A novel Lyapunov functional is constructed to establish a criterion to ensure some certain H_∞ performance of the closed-loop system. This Lyapunov functional is dependent on the integral of the state error involved in the event-triggered scheme. (iii) Under the event-triggered sampling scheme, suitable state-feedback controllers can be designed rather than be given a priori. Moreover, a self-triggered implementation of the proposed event-triggered sampling scheme is presented as well. Finally, a batch reactor model and an inverted pendulum system are given to demonstrate the effectiveness of the proposed method.

Keywords event-triggered sampling, self-triggered implementation, H_∞ control, looped-functional

1 Introduction

Sampled-data control systems have been studied for over seven decades, and have played a crucial role in modern advanced control dominated by digitalized technologies [1–7]. One of critical issues is how to sample those 'necessary' signals such that some certain system performance can be 'retained'. Compared with the traditional time-triggered sampling (periodic sampling or non-periodic sampling), event-triggered sampling is demonstrated to be a natural way to choose necessary signals to be sampled [8,9]. Since the original work [10] was reported, event-triggered sampling has become a hot topic and a large number of results have been published in [11–18].

To devise an event-triggered sampling scheme, the predefined event-triggering condition is fundamental for choosing necessary signals to sample. Recalling some existing results, there are two classes of event-triggering conditions. To make it clear, let $x(t)$ and $x(t_k)$ be the current state and the sampled state at the latest time instant t_k ($k \in \mathbb{Z}_{\geqslant 0}$), respectively. Let $\Delta x(t) = x(t) - x(t_k)$ be the state increment. The event-triggering condition is represented as $f(x, \Delta x) > 0$.

We refer to the first class of event-triggering conditions as relative error (in the sense of a vector norm) conditions. A typical example reads as follows [10]:

$$f(x, \Delta x) = f_1(x, \Delta x) > 0, \tag{1a}$$

$$f_1(x, \Delta x) = [\Delta x(t)]^{\mathrm{T}} \Omega [\Delta x(t)] - \delta x^{\mathrm{T}}(t) \Omega x(t), \tag{1b}$$

where, hereafter, Ω is a weighted real symmetric positive definite matrix, and $\delta > 0$ is a threshold. Clearly, the condition (1) is checked through calculating the state increment $\Delta x(t)$. Once the relative

* Corresponding author (email: qhan@swin.edu.au)

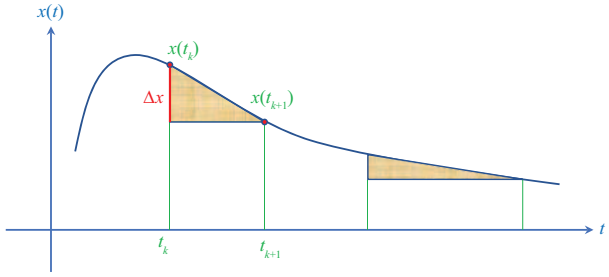

Figure 1 (Color online) Diagram for the event-triggering condition (3).

error $\tilde{e}(t) := \|\Omega^{\frac{1}{2}}\Delta x(t)\|/\|\Omega^{\frac{1}{2}}x(t)\|$ is greater than $\sqrt{\delta}$, the current state $x(t)$ is sampled. However, when the system state varies slowly enough, the relative error $\tilde{e}(t)$ may not be greater than $\sqrt{\delta}$ for a long time. As a result, those necessary signals for the sampled-data system are not sampled. Some other existing relative-error-based conditions exhibit the same feature albeit in different forms [19].

The second class of event-triggering conditions are integral-based event-triggering conditions. For example, in [20], it is suggested that

$$f(x,\Delta x) = f_2(x,\Delta x) > 0, \tag{2a}$$

$$f_2(x,\Delta x) = \int_{t_k}^{t} [\Delta x(s)]^{\mathrm{T}}\Omega[\Delta x(s)]\mathrm{d}s - \int_{t_k}^{t} \delta x^{\mathrm{T}}(s)\Omega x(s)\mathrm{d}s. \tag{2b}$$

The condition (2) works through comparing the accumulation of the weighted state increment $\|\Omega^{\frac{1}{2}}[\Delta x(s)]\|$ with the accumulation of the weighted state $\sqrt{\delta}\|\Omega^{\frac{1}{2}}x(s)\|$ over the time interval $[t_k, t]$. This condition can be regarded as an extension of (1). Since the variation tendencies of Δx and x are the same, when the system state varies slowly enough, this condition may be difficult to be satisfied for a long time, similar to the first class of event-triggering conditions. Some other integral-based event-triggering conditions can be found in [21], whose intrinsic feature is the same as that of (2).

From the analysis above, our intuition suggests the following event-triggering condition:

$$f(x,\Delta x) = f_3(x,\Delta x) > 0, \tag{3a}$$

$$f_3(x,\Delta x) = \left[\int_{t_k}^{t} \Delta x(s)\mathrm{d}s\right]^{\mathrm{T}} \Omega \left[\int_{t_k}^{t} \Delta x(s)\mathrm{d}s\right] - \delta x^{\mathrm{T}}(t_k)\Omega x(t_k). \tag{3b}$$

A physical explanation of the condition (3) is given in Figure 1. This condition compares the accumulation (the shadow part in the figure) of the state increment $\Delta x(s)$ over the interval $[t_k, t]$ with the latest sampled state $x(t_k)$. It is more natural and effective than (1) and (3) in the event-triggered sampling, especially when the system state fluctuates in a very small range. Nevertheless, some questions arise as follows.

(a) Does the condition (3) work better compared with the conditions (1) and (2)? Can the Zeno behaviour be excluded?

(b) How to deal with the condition (3) in the stability analysis of sampled-data systems? Note that $x(t_k)$ appears both inside and outside the integral involved, which is not easy to deal with.

(c) How to implement the related event-triggered scheme (ETS) if no extra device is available to monitor the system state?

Answering these questions is the first motivation of the study.

On the other hand, most of the results on event-triggered control are based on an emulation method [10, 22]. That is, for the given system performance, a suitable controller is designed in advance. Then an event-triggering condition is predefined to sample the system state such that the resultant sampled-data system can retain the system performance. It is clear that the controller designed is independent of event-triggered sampling. In other words, the controller cannot reflect characteristics inherited from event-triggered sampling. Although some algorithms are provided in [23–25] to design suitable event-triggered state feedback controllers, event-triggered sampling is not involved, that is, system states are sampled periodically rather than event-triggered. As such, a question arises: is it possible to design a controller that is dependent on event-triggered sampling? Answering this question is the second motivation of the study.

This paper provides positive answers to the questions above. First, we prove that the event-triggering condition (3) works pretty well in the sense that it can avoid the so-called Zeno behaviour. Second, the vector $\int_{t_k}^{t} \Delta x(s)\mathrm{d}s$ is used to construct a novel Lyapunov functional, which builds up a bridge between the event-triggering condition and the H_∞ performance analysis of the closed-loop system associated with a state feedback controller. With the novel Lyapunov functional, a sufficient condition to ensure the desired H_∞ gain performance is obtained using a looped functional method. Third, based on the obtained sufficient condition, an algorithm is presented to co-design the state feedback controller and the weighting matrix Ω in the event-triggering condition (3). Moreover, a self-triggered mechanism is presented to implement the proposed ETS. Simulation results finally demonstrate the effectiveness of the proposed method.

Notations. The notations throughout this paper are standard. $\mathrm{diag}\{\cdots\}$ and $\mathrm{col}\{\cdots\}$ denote a block-diagonal matrix and a block-column matrix (vector), respectively. The symbol '$\star$' in a symmetric block matrix stands for a term induced by symmetry. $\mathbb{Z}_{\geqslant}0$ means the set of non-negative integers. $\mathcal{L}_2[t_0,\infty)$ denotes the space of square-integrable vector functions over $[t_0,\infty)$. $\mathrm{He}\{X\} = X + X^{\mathrm{T}}$.

2 A novel ETS

Consider the linear time-variant system described by

$$\begin{cases} \dot{x}(t) = Ax(t) + Bu(t) + Dw(t),\ x(t_0) = x_0, \\ z(t) = Cx(t) + Eu(t) + Fw(t), \end{cases} \tag{4}$$

where $x \in \mathbb{R}^n$, $u \in \mathbb{R}^m$, $z \in \mathbb{R}^p$, and $w \in \mathbb{R}^r$ are the system state, the control input, the controlled output, and the external disturbance with $w \in \mathcal{L}_2[t_0,\infty)$, respectively. The real matrices A, B, C, D, E and F are known with compatible dimensions, and x_0 is an initial state of the system.

Suppose that the system state is measurable and thus a suitable state feedback control $u(t) = Kx(t)$ can be performed, where K is a real matrix to be designed. In order to calculate control signals, the system state $x(t)$ is sampled at time instants $\{t_1, t_2, \ldots, t_k, \ldots\}$ in an event-triggered pattern [10], leading to the following closed-loop system:

$$\begin{cases} \dot{x}(t) = Ax(t) + BKx(t_k) + Dw(t),\ x(t_0) = x_0, \\ z(t) = Cx(t) + EKx(t_k) + Fw(t), \quad t \in [t_k, t_{k+1}). \end{cases} \tag{5}$$

Let t_k be the latest sampling instant. The event-triggered pattern determines the next sampling instant t_{k+1} not by a lapse of time but by a predefined event-triggering condition. Different from the existing ones, we consider a novel event-triggering condition $f(x,\Delta x) = f_3(x,\Delta x)$, where $f_3(x,\Delta x)$ is defined in (3). Then, the ETS is given by, for $t_0 = 0$ and $k \in \mathbb{Z}_{\geqslant}0$

$$t_{k+1} = \inf\big\{t > t_k |\ f_3(x,\Delta x) > 0\big\}. \tag{6}$$

An important issue on the event-triggered sampling is the so-called 'Zeno' behaviour, which means that $\lim_{k\to\infty} t_k < \infty$. To exclude the Zeno behaviour, the minimal inter-event time should be greater than zero. For the proposed event-triggering condition (6), the following theorem discloses that the Zeno behaviour can be excluded. For this goal, we need Assumption 1.

Assumption 1. For the system (4), the disturbance w satisfies $\|w\| \leqslant c_w\|x\|$, where c_w is a positive scalar.

Theorem 1. Under Assumption 1, the ETS (6) ensures that the Zeno behaviour is excluded for the closed-loop system (5).

Proof. Without loss of generality, we suppose $x(t_k) \neq 0$. If $x(t_k) = 0$, then the system reaches its steady state. In this situation, no triggers are needed. From the event-triggering condition (3a), $f_3(x,\Delta x) > 0$ can be rewritten as

$$\sqrt{\delta}\|\Omega^{\frac{1}{2}}x(t_k)\| < \left\|\Omega^{\frac{1}{2}}\int_{t_k}^{t}\Delta x(s)\mathrm{d}s\right\|. \tag{7}$$

By the Taylor expansion, we have

$$\Delta x(t) = x(t) - x(t_k) = \dot{x}(t_k)(t - t_k) + o(t - t_k), \tag{8}$$

where $o(t - t_k)$ is infinitesimal as $t - t_k \to 0^+$ and $\lim_{t\to t_k^+} \frac{o(t-t_k)}{t-t_k} = 0$. Then, we obtain

$$\begin{aligned}\left\|\Omega^{\frac{1}{2}} \int_{t_k}^{t} \Delta x(s)\mathrm{d}s\right\| &= \left\|\Omega^{\frac{1}{2}} \int_{t_k}^{t} [\dot{x}(t_k)(s - t_k) + o(s - t_k)]\mathrm{d}s\right\| \\ &\leqslant \left\|\Omega^{\frac{1}{2}} \int_{t_k}^{t} \dot{x}(t_k)(s - t_k)\mathrm{d}s\right\| + \int_{t_k}^{t} \|\Omega^{\frac{1}{2}} o(s - t_k)\|\mathrm{d}s. \end{aligned} \tag{9}$$

We now prove the conclusion by contradiction. Suppose that the Zeno behaviour occurs, that is, $\lim_{k\to\infty} t_k < \infty$. Then for any $\epsilon > 0$, there exists a certain integer k_0 sufficiently large such that for $k > k_0$,

$$t_{k+1} - t_k \leqslant \epsilon \leqslant \epsilon_0, \tag{10}$$

where $\epsilon_0 > 0$ is given later. Let $\epsilon > 0$ be sufficiently small. We estimate $\|\Omega^{\frac{1}{2}} o(t - t_k)\|$ for $t \in [t_k, t_k + \epsilon]$. Due to $\lim_{t\to t_k^+} \frac{o(t-t_k)}{t-t_k} = 0$, it is clear that $\lim_{t\to t_k^+} \frac{\|\Omega^{\frac{1}{2}} o(t-t_k)\|}{t-t_k} = 0$. Then there exists a proper positive number ρ_0 such that

$$\|\Omega^{\frac{1}{2}} o(t - t_k)\| \leqslant \rho_0 \|\Omega^{\frac{1}{2}} x(t_k)\|(t - t_k), \quad \forall t \in [t_k, t_k + \epsilon]. \tag{11}$$

Let

$$\epsilon_0 = \sqrt{2\sqrt{\delta}/(\wp_0 + \rho_0)}, \tag{12}$$

$$\wp_0 = \|\Omega^{\frac{1}{2}}(A + BK)\Omega^{-\frac{1}{2}}\| + c_w \|\Omega^{\frac{1}{2}} D\Omega^{-\frac{1}{2}}\|. \tag{13}$$

Substituting (11) into (9), we have

$$\left\|\Omega^{\frac{1}{2}} \int_{t_k}^{t} \Delta x(s)\mathrm{d}s\right\| \leqslant \frac{1}{2}\big[\|\Omega^{\frac{1}{2}} \dot{x}(t_k)\| + \rho_0 \|\Omega^{\frac{1}{2}} x(t_k)\|\big](t - t_k)^2. \tag{14}$$

Hence, following (14) and (7) yields

$$(t_{k+1} - t_k)^2 > \frac{2\sqrt{\delta}\|\Omega^{\frac{1}{2}} x(t_k)\|}{\|\Omega^{\frac{1}{2}} \dot{x}(t_k)\| + \rho_0 \|\Omega^{\frac{1}{2}} x(t_k)\|}. \tag{15}$$

Note from (5) that

$$\|\Omega^{\frac{1}{2}} \dot{x}(t_k)\| = \big\|\Omega^{\frac{1}{2}}[(A + BK)x(t_k) + Dw(t_k)]\big\|. \tag{16}$$

Under Assumption 1, we have

$$\|\Omega^{\frac{1}{2}} \dot{x}(t_k)\| \leqslant \wp_0 \|\Omega^{\frac{1}{2}} x(t_k)\|. \tag{17}$$

Thus, substituting (17) into (15) gives $t_{k+1} - t_k > \epsilon_0$, which is in contradiction with (10). The proof is completed.

Remark 1. From Theorem 1, one can see that the proposed ETS (6) can exclude Zeno behaviours. In fact, for a certain $\rho_0 > 0$, the minimum inter-event time is greater than a positive number ϵ_0 given explicitly in (12). Moreover, the proof of Theorem 1 can also motivate a self-triggered implementation of the proposed ETS, which can be seen in Section 3.

Remark 2. Compared with some existing ETSs with (1), the minimum inter-event time from the ETS (6) should be strictly greater than zero since it takes time for the accumulation $\|\Omega^{\frac{1}{2}} \int_{t_k}^{t} [\Delta x(s)]\mathrm{d}s\|$ to reach the value of $\sqrt{\delta}\|\Omega^{\frac{1}{2}} x(t_k)\|$.

3 Application to H_∞ control

3.1 Problem statement

When the system state is little fluctuating such that no event will be triggered, the performance of a control system may be degraded due to the fact that no control signal is updated. Moreover, if this case happens, the sampling interval $t_{k+1}-t_k$ may go to infinity, which makes it difficult to detect sensor failures. In this situation, the ETS can be equipped with a timeout mechanism such that the maximum sampling interval is less than a constant $T_{\max}>0$ [26]. Bearing that in mind, the ETS (6) is adapted to the following, for $t_0=0$ and $k\in\mathbb{Z}_{\geqslant 0}$

$$t_{k+1}=\min\{\inf\{t>t_k|f_3(x,\Delta x)>0\},t_k+T_{\max}\}. \tag{18}$$

Under the ETS (18), it is ensured that $t_{k+1}-t_k\leqslant T_{\max}$. By Theorem 1, there exists a positive real number $T_{\min}>0$ such that $t_{k+1}-t_k\geqslant T_{\min}$ for $k\in\mathbb{Z}_{\geqslant 0}$. Thus, we have

$$T_{\min}\leqslant t_{k+1}-t_k\leqslant T_{\max},\ k\in\mathbb{Z}_{\geqslant 0}. \tag{19}$$

The event-triggered H_∞ control problem to be addressed in this paper is stated as follows.

OP1: For a given scalar $\gamma>0$, let a performance index be defined by

$$J=\int_{t_0}^{\infty}[z^{\mathrm{T}}(t)z(t)-\gamma^2 w^{\mathrm{T}}(t)w(t)]\mathrm{d}t. \tag{20}$$

Under the ETS (18), co-design a suitable control gain K and the weighting matrix Ω such that the closed-loop system (5) is internally asymptotically stable and $J<0$ under the zero initial condition $x_0=0$.

3.2 Solving the problem OP1

In this subsection, we provide a solution to the problem OP1. Note that the closed-loop system (5) is a sampled-data system with the constraint $f_3(x,\Delta x)\leqslant 0,\ t\in[t_k,t_{k+1})$. Let

$$\upsilon_1(t)=\int_{t_k}^{t}[x(s)-x(t_k)]\mathrm{d}s. \tag{21}$$

Then for $t\in[t_k,t_{k+1})$, the constraint $f_3(x,\Delta x)\leqslant 0$ can be rewritten as follows:

$$\upsilon_1^{\mathrm{T}}(t)\Omega\upsilon_1(t)\leqslant\delta x^{\mathrm{T}}(t_k)\Omega x(t_k),\quad t\in[t_k,t_{k+1}). \tag{22}$$

We employ the looped functional method [27] to analyze the H_∞ performance of (5). In doing so, we choose a novel Lyapunov functional as follows:

$$\mathcal{W}(t)=V(t)+\mathcal{V}_0(t), \tag{23}$$

where $V(t)=x^{\mathrm{T}}(t)Px(t)$ with $P>0$ and

$$\begin{aligned}\mathcal{V}_0(t)=&2\begin{bmatrix}x(t)\\x(t_k)\\x(t_{k+1})\\\upsilon_1(t)\\\upsilon_2(t)\end{bmatrix}^{\mathrm{T}}Q_1\begin{bmatrix}(t_{k+1}-t)[x(t)-x(t_k)]\\(t_{k+1}-t)\upsilon_1(t)\\(t-t_k)[x(t_{k+1})-x(t)]\\(t-t_k)\upsilon_2(t)\end{bmatrix}\\&+2\begin{bmatrix}x(t)-x(t_k)\\\upsilon_1(t)\end{bmatrix}^{\mathrm{T}}Q_2\begin{bmatrix}x(t_{k+1})-x(t)\\\upsilon_2(t)\end{bmatrix}+(t_{k+1}-t)(t-t_k)\begin{bmatrix}x(t_k)\\x(t_{k+1})\end{bmatrix}^{\mathrm{T}}Q_3\begin{bmatrix}x(t_k)\\x(t_{k+1})\end{bmatrix}\\&+(t_{k+1}-t)\int_{t_k}^{t}\dot{x}^{\mathrm{T}}(s)R_1\dot{x}(s)\mathrm{d}s-(t-t_k)\int_{t}^{t_{k+1}}\dot{x}^{\mathrm{T}}(s)R_2\dot{x}(s)\mathrm{d}s,\quad t\in[t_k,t_{k+1})\end{aligned} \tag{24}$$

with $R_1>0$, $R_2>0$; Q_i $(i=1,2,3)$ are real matrices of compatible dimensions with $Q_3=Q_3^{\mathrm{T}}$ and $\upsilon_2(t)=\int_t^{t_{k+1}}x(s)\mathrm{d}s$.

Remark 3. Since $\mathcal{V}_0(t_k) = \mathcal{V}_0(t_{k+1}) = 0$, $\mathcal{V}_0(t)$ is a looped functional. One of its significant features is that it takes the ETS (18) into account due to the introduction of $\upsilon_1(t)$ in (21). Thus, the looped functional (24) builds a bridge between the proposed ETS and the H_∞ performance analysis of the system (5). This feature enables us to design an ETS-dependent control gain K.

In what follows, we first analyze the H_∞ performance for the closed-looped system (5) to obtain a sufficient condition on $J < 0$ using the looped functional method. Then, this condition is employed to co-design the event-triggered parameter Ω and the control gain K.

3.2.1 H_∞ *performance analysis*

Let $e_i \in \mathbb{R}^{n\times 8n}$ $(i = 1, 2, \ldots, 8)$ be row-block vectors taken from the $8n$-dimensional identity matrix successively from its top to its bottom. Then we state and establish the following result based on the Lyapunov functional (23).

Proposition 1. For given constants $\gamma > 0$, $\delta > 0$ and a real matrix $\Omega > 0$, the closed-loop system (5) is internally asymptotically stable and $J < 0$ for $x_0 = 0$ if there exist real matrices $P > 0$, $R_1 > 0$, $R_2 > 0$, real symmetric matrices Q_2, Q_3, and real matrices Q_1, $\mathcal{M}_1$, $\mathcal{M}_2$, N_1, N_2, N_3 with appropriate dimensions such that, for $T_k \in \{T_{\min}, T_{\max}\}$

$$\beth_1 \triangleq \begin{bmatrix} \beth_{11} & N_3^{\mathrm{T}}D & L_0^{\mathrm{T}} & T_k\mathcal{M}_2^{\mathrm{T}} \\ \star & -\gamma^2 I & F^{\mathrm{T}} & 0 \\ \star & \star & -I & 0 \\ \star & \star & \star & -T_k\mathcal{R}_2 \end{bmatrix} < 0, \tag{25}$$

$$\beth_2 \triangleq \begin{bmatrix} \beth_{21} & N_3^{\mathrm{T}}D & L_0^{\mathrm{T}} & T_k\mathcal{M}_1^{\mathrm{T}} \\ \star & -\gamma^2 I & F^{\mathrm{T}} & 0 \\ \star & \star & -I & 0 \\ \star & \star & \star & -T_k\mathcal{R}_1 \end{bmatrix} < 0, \tag{26}$$

where $L_0 = Ce_2 + EKe_3$, $\mathcal{R}_i = \mathrm{diag}\{R_i, 3R_i\}$ $(i = 1, 2)$, and

$$\beth_{11} = \Phi_1 + \Phi_2 + T_k[\Gamma_1 - \mathrm{He}\{N_2^{\mathrm{T}}e_8\}], \tag{27}$$

$$\beth_{21} = \Phi_1 + \Phi_2 + T_k[\Gamma_2 + \mathrm{He}\{N_1^{\mathrm{T}}(e_3 - e_7)\}], \tag{28}$$

$$\Phi_1 = \mathrm{He}\big\{e_2^{\mathrm{T}}Pe_1 + C_1^{\mathrm{T}}Q_1C_{20} + C_{51}^{\mathrm{T}}Q_2C_{61} - C_{52}^{\mathrm{T}}Q_2C_{62} + \mathcal{M}_1^{\mathrm{T}}\Theta\mathscr{C}_1 + \mathcal{M}_2^{\mathrm{T}}\Theta\mathscr{C}_2\big\}, \tag{29}$$

$$\Phi_2 = \delta e_3^{\mathrm{T}}\Omega e_3 - e_5^{\mathrm{T}}\Omega e_5 + \mathrm{He}\{N_1^{\mathrm{T}}e_5 + N_2^{\mathrm{T}}e_6 + N_3^{\mathrm{T}}C_0\}, \tag{30}$$

$$\Gamma_1 = \mathrm{He}\{C_1^{\mathrm{T}}Q_1C_{22} + C_3^{\mathrm{T}}Q_1C_{42}\} + C_7^{\mathrm{T}}Q_3C_7 + e_1^{\mathrm{T}}R_1e_1, \tag{31}$$

$$\Gamma_2 = \mathrm{He}\{C_1^{\mathrm{T}}Q_1C_{21} + C_3^{\mathrm{T}}Q_1C_{41}\} + e_1^{\mathrm{T}}R_2e_1 - C_7^{\mathrm{T}}Q_3C_7 \tag{32}$$

with $\Theta := \left[\begin{smallmatrix} I & -I & 0 \\ I & I & -2I \end{smallmatrix}\right]$, and

$$\begin{aligned}
&\mathscr{C}_1 = \mathrm{col}\{e_2, e_3, e_7\}, \quad \mathscr{C}_2 = \mathrm{col}\{e_4, e_2, e_8\}, \\
&C_0 = -e_1 + Ae_2 + BKe_3, \quad C_1 = \mathrm{col}\{e_2, e_3, e_4, e_5, e_6\}, \\
&C_{20} = \mathrm{col}\{e_3 - e_2, -e_5, e_4 - e_2, e_6\}, \quad C_{21} = \mathrm{col}\{0, 0, -e_1, -e_2\}, \\
&C_{22} = \mathrm{col}\{e_1, e_2 - e_3, 0, 0\}, \quad C_3 = \mathrm{col}\{e_1, 0, 0, e_2 - e_3, -e_2\}, \\
&C_{41} = \mathrm{col}\{0, 0, e_4 - e_2, e_6\}, \quad C_{42} = \mathrm{col}\{e_2 - e_3, e_5, 0, 0\}, \\
&C_{51} = \mathrm{col}\{e_1, e_2 - e_3\}, \quad C_{52} = \mathrm{col}\{e_2 - e_3, e_5\}, \\
&C_{61} = \mathrm{col}\{e_4 - e_2, e_6\}, \quad C_{62} = \mathrm{col}\{e_1, e_2\}, \quad C_7 = \mathrm{col}\{e_3, e_4\}.
\end{aligned}$$

Proof. See Appendix A.

Remark 4. Proposition 1 presents a novel sufficient condition to ensure the asymptotic stability and $J < 0$ for the closed-loop system (5) under the proposed ETS, thanks to the looped functional (24). Furthermore, another significant advantage of Proposition 1 is that it can be also used to co-design the control gain K and the weighting matrix Ω, which is shown in Subsection 3.2.2.

3.2.2 *Co-design of the gain K and the weighting matrix Ω*

Note that the matrix inequalities in Proposition 1 are nonlinear due to that the matrix variables N_3 and K are coupled in the term $N_3^{\mathrm{T}}BKe_3$ in Φ_2. A parameter tuning method [28] can be employed to decouple them.

Proposition 2. For given constants $\gamma > 0$, $\delta > 0$ and real scalars ϵ_i $(i = 1, 2)$, the H_∞ control problem OP1 is solvable with $K = YX^{-1}$ if there exist real matrices $\tilde{\Omega} > 0$, $\bar{P} > 0$, $\bar{R}_1 > 0$, $\bar{R}_2 > 0$, real symmetric matrices $\bar{Q}_2$, $\bar{Q}_3$, and real matrices $\bar{Q}_1$, $\tilde{\mathcal{M}}_1$, $\tilde{\mathcal{M}}_2$, $\bar{N}_1$, $\bar{N}_2$, X and Y with appropriate dimensions such that, for $T_k \in \{T_{\min}, T_{\max}\}$

$$\begin{bmatrix} \tilde{\Xi}_{11} & \star & \star & \star \\ D^{\mathrm{T}}\Im_0 & -\gamma^2 I & \star & \star \\ CXe_2 + EYe_3 & F & -I & \star \\ T_k\tilde{\mathcal{M}}_2 & 0 & 0 & -T_k\tilde{\mathcal{R}}_2 \end{bmatrix} < 0, \tag{33}$$

$$\begin{bmatrix} \tilde{\Xi}_{21} & \star & \star & \star \\ D^{\mathrm{T}}\Im_0 & -\gamma^2 I & \star & \star \\ CXe_2 + EYe_3 & F & -I & \star \\ T_k\tilde{\mathcal{M}}_1 & 0 & 0 & -T_k\tilde{\mathcal{R}}_1 \end{bmatrix} < 0, \tag{34}$$

where $\Im_0 = e_1 + \epsilon_1 e_2 + \epsilon_2 e_3$, $\tilde{R}_i = \mathrm{diag}\{\bar{R}_i, 3\bar{R}_i\}$, and

$$\begin{aligned}
\tilde{\Xi}_{11} &= \tilde{\Phi}_1 + \tilde{\Phi}_2 + T_k[\tilde{\Gamma}_1 - \mathrm{He}\{\bar{N}_2^{\mathrm{T}}e_8\}], \\
\tilde{\Xi}_{21} &= \tilde{\Phi}_1 + \tilde{\Phi}_2 + T_k[\tilde{\Gamma}_2 + \mathrm{He}\{\bar{N}_1^{\mathrm{T}}(e_3 - e_7)\}], \\
\tilde{\Phi}_1 &= \mathrm{He}\{e_2^{\mathrm{T}}\bar{P}e_1 + C_1^{\mathrm{T}}\bar{Q}_1C_{20} + C_{51}^{\mathrm{T}}\bar{Q}_2C_{61} - C_{52}^{\mathrm{T}}\bar{Q}_2C_{62} + \tilde{\mathcal{M}}_1^{\mathrm{T}}\Theta\mathscr{C}_1 + \tilde{\mathcal{M}}_2^{\mathrm{T}}\Theta\mathscr{C}_2\}, \\
\tilde{\Phi}_2 &= \delta e_3^{\mathrm{T}}\tilde{\Omega}e_3 - e_5^{\mathrm{T}}\tilde{\Omega}e_5 + \mathrm{He}\{\bar{N}_1^{\mathrm{T}}e_5 + \bar{N}_2^{\mathrm{T}}e_6 + \Im_0^{\mathrm{T}}(-Xe_1 + AXe_2 + BYe_3)\}, \\
\tilde{\Gamma}_1 &= \mathrm{He}\{C_1^{\mathrm{T}}\bar{Q}_1C_{22} + C_3^{\mathrm{T}}\bar{Q}_1C_{42}\} + C_7^{\mathrm{T}}\bar{Q}_3C_7 + e_1^{\mathrm{T}}\bar{R}_1e_1, \\
\tilde{\Gamma}_2 &= \mathrm{He}\{C_1^{\mathrm{T}}\bar{Q}_1C_{21} + C_3^{\mathrm{T}}\bar{Q}_1C_{41}\} + e_1^{\mathrm{T}}\bar{R}_2e_1 - C_7^{\mathrm{T}}\bar{Q}_3C_7,
\end{aligned}$$

and the other notations are defined in Proposition 1.

Proof. See Appendix B.

Remark 5. Proposition 2 gives a sufficient condition to co-design both the control gain K and the weighting matrix Ω in the ETS (18). If the linear matrix inequalities (33) and (34) are feasible, a suitable solution to $(\Omega, K) = (YX^{-1}, X^{-\mathrm{T}}\bar{\Omega}X^{-1})$ can be obtained. Recalling some existing results on event-triggered sampling [10, 22], an emulation-based method is commonly employed. In this method, a controller is initially designed, followed by the development of a suitable event-triggered sampling scheme. This sequence ensures the maintenance of specific system performance. Clearly, it is advantageous if both a controller and an event-triggered sampling scheme can be co-designed, as done in this paper. This not only simplifies the design process of the emulation-based method but also facilitates the satisfaction of desired system performance through the design of an event-triggered-dependent controller.

Remark 6. Proposition 2 introduces several parameters, including λ, δ, ϵ_1, ϵ_2, $T_{\min}$, and $T_{\max}$. The parameter λ represents a prescribed H_∞ performance level, while δ serves as a threshold for triggering events, typically taking values between 0 and 1. A smaller δ may result in a higher frequency of triggered events. The matrix inequalities (33) and (34) imply that the parameter $T_{\min}$ must be strictly greater than zero. For practical applications, a common choice is to set $T_{\min} = 10^{-5}$, as done in [27].

According to Proposition 2, it is possible to maximize $T_{\max}$ by adjusting ϵ_1 and ϵ_2 such that the matrix inequalities (33) and (34) remain feasible. Therefore, ϵ_1 and ϵ_2 become two tuning parameters. Utilizing a numerical optimization algorithm, such as fminsearch in the optimization toolbox, allows for the identification of an optimal combination of these parameters.

3.3 Self-triggered implementation of the ETS (18)

It is clear that the ETS (18) relies on an extra device to continuously monitor the system state, leading to a complicated realization of it. However, inspiring from the proof of Theorem 1, a self-triggered

implementation scheme can be designed. In fact, from the proof of Theorem 1, one can see that

$$\sqrt{\delta}\|\Omega^{\frac{1}{2}}x(t_k)\| < \left\|\Omega^{\frac{1}{2}}\int_{t_k}^{t}\dot{x}(t_k)(s-t_k)\mathrm{d}s\right\| + \int_{t_k}^{t}\|\Omega^{\frac{1}{2}}o(s-t_k)\|\mathrm{d}s. \tag{35}$$

Note that there exists a positive scalar β_0 such that

$$\|\Omega^{\frac{1}{2}}o(t-t_k)\| \leqslant \beta_0\|\Omega^{\frac{1}{2}}x(t_k)\|(t-t_k),\ t\in[t_k,t_{k+1}]. \tag{36}$$

Substituting (36) to (35) yields

$$(t_{k+1}-t_k)^2 > \frac{2\sqrt{\delta}\|\Omega^{\frac{1}{2}}x(t_k)\|}{\|\Omega^{\frac{1}{2}}\dot{x}(t_k)\|+\beta_0\|\Omega^{\frac{1}{2}}x(t_k)\|}. \tag{37}$$

Under Assumption 1, together with (16), it is clear that

$$\|\Omega^{\frac{1}{2}}\dot{x}(t_k)\| \leqslant \aleph(x(t_k)),$$

where $\aleph(x(t_k)) = \|\Omega^{\frac{1}{2}}(A+BK)x(t_k)\| + c_w\|\Omega^{\frac{1}{2}}D\|\|x(t_k)\|$. Thus, from (37), one has that

$$t_{k+1}-t_k > \sqrt{g(x(t_k))}, \tag{38}$$

where

$$g(x(t_k)) = \frac{2\sqrt{\delta}\|\Omega^{\frac{1}{2}}x(t_k)\|}{\aleph(x(t_k))+\beta_0\|\Omega^{\frac{1}{2}}x(t_k)\|}.$$

Note that $g(x(t_k))$ is dependent just on the system state at t_k. Therefore, a self-triggered scheme (STS) to implement the ETS (18) is readily devised.

Self-triggered implementation. For the system (5) with the control gain K obtained from Proposition 2, under Assumption 1, a self-triggered implementation of the ETS (18) can be described as, for $t_0=0$ and $k\in\mathbb{Z}_{\geqslant 0}$

$$\text{STS:}\ \ t_{k+1} = t_k + \min\{\eta\sqrt{g(x(t_k))}, T_{\max}\},\ \eta\geqslant 1. \tag{39}$$

Remark 7. The scheme (39) presents a self-triggered implementation of the ETS (18) for the system (5). Similar to the proof of Theorem 1, this scheme can also exclude the Zeno behaviour. In fact, it is not difficult to prove that $g(x(t_k)) \geqslant 2\sqrt{\delta}/(\wp_1+\beta_0)$ due to $\aleph(x(t_k)) \leqslant \wp_1\|\Omega^{\frac{1}{2}}x(t_k)\|$, where $\wp_1 = \|\Omega^{\frac{1}{2}}(A+BK)\Omega^{\frac{-1}{2}}\| + c_w\|\Omega^{\frac{1}{2}}D\|\|\Omega^{\frac{-1}{2}}\|$, which means that $t_{k+1}-t_k \geqslant 2\sqrt{\delta}/(\wp_1+\beta_0) > 0$, $\forall k\in\mathbb{Z}_{\geqslant 0}$. By Proposition 1, for a given K, we can calculate the allowable maximum $T_{\max}$ such that the closed-loop system (5) is asymptotically stable with a prescribed H_∞ level. Thus, the introduction of the parameter η is to ensure $t_{k+1}-t_k \in [\sqrt{g(x(t_k))}, T_{\max}]$ for $\forall k\in\mathbb{Z}_{\geqslant 0}$. In practical applications, one can take a value of η close to one, say, $\eta=1.01$ as a tradeoff between less triggered events and the desired system performance.

4 Illustrative examples

In this section, we take a batch reactor model and an inverted pendulum model to demonstrate the effectiveness of the proposed ETS and the co-design method.

Example 1. Consider the batch reactor model from [29], whose state space description is given as (4) with

$$A = \begin{bmatrix} 1.38 & -0.2 & 6.71 & -5.67 \\ -0.58 & -4.29 & 0 & 0.67 \\ 1.06 & 4.27 & -6.65 & 5.89 \\ 0.04 & 4.27 & 1.34 & -2.1 \end{bmatrix},\quad B = \begin{bmatrix} 0 & 0 \\ 5.67 & 0 \\ 1.13 & -3.14 \\ 1.13 & 0 \end{bmatrix},$$

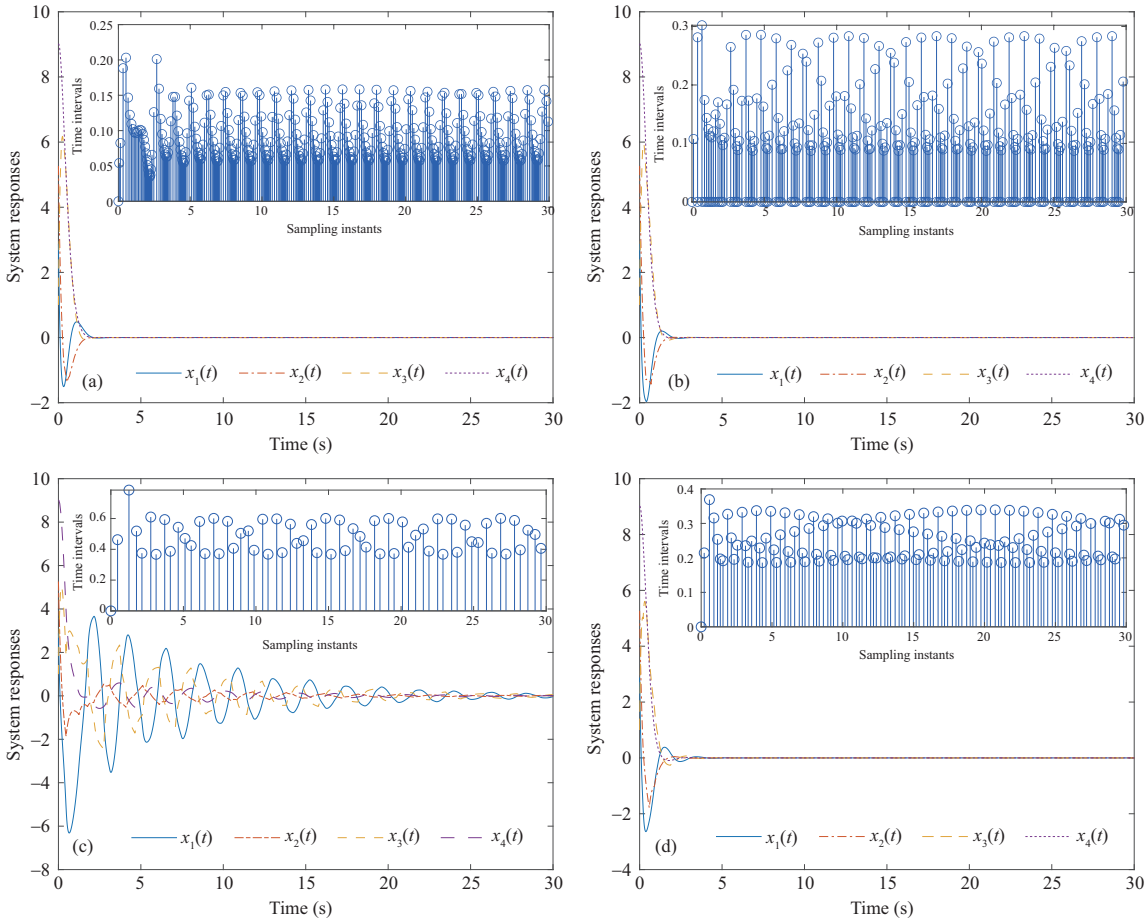

Figure 2 (Color online) State responses and time-intervals with (a) ETS1, (b) ETS2, (c) ETS3, and (d) ETS3a.

Table 1 Comparison among ETS1, ETS2 and ETS3

	Number of events	Average time (s)	Minimum time (s)
ETS1	329	0.0909	0.0348
ETS2	340	0.08763	0.0001
ETS3	62	0.4781	0.3675
ETS3a	119	0.2506	0.1862
STS	87	0.3443	0.2594
$\text{STS}_{\eta=1.2}$	73	0.4075	0.2844

and $D = \text{col}\{1, 1, 1, 1\}$. We take the control gain K from [30]

$$K = \begin{bmatrix} 0.1006 & -0.2469 & -0.0952 & -0.2447 \\ 1.4099 & -0.1966 & 0.0139 & 0.0823 \end{bmatrix}.$$

Suppose that the disturbance $w(t)$ is given as $w(t) = 0.01\sqrt{x^{\mathrm{T}}(t)x(t)}$, and that the initial state is set as $x_0 = \text{col}\big\{6\sin(0.5), 6\cos(0.5), 1, 9\big\}$.

For this example, we compare the relative-based ETS (1), the integral-based ETS (2) and the proposed ETS (18). For convenience, we rename them as ETS1, ETS2 and ETS3, respectively, and let $\delta = 0.1$ and $\Omega = I$. With ETS1, ETS2 and ETS3, the state responses of the closed-loop system (5) and the time intervals between two consecutive events are plotted in Figures 2(a)–(c), respectively.

Based on these simulation results, we calculate the number of events triggered, the average sampling period and the minimum event time during $[0, 30]$ s with different ETSs, and the obtained results are listed in Table 1. From this table, one can find the following.

- The proposed ETS3 triggers the least number of events, leading to the largest average sampling

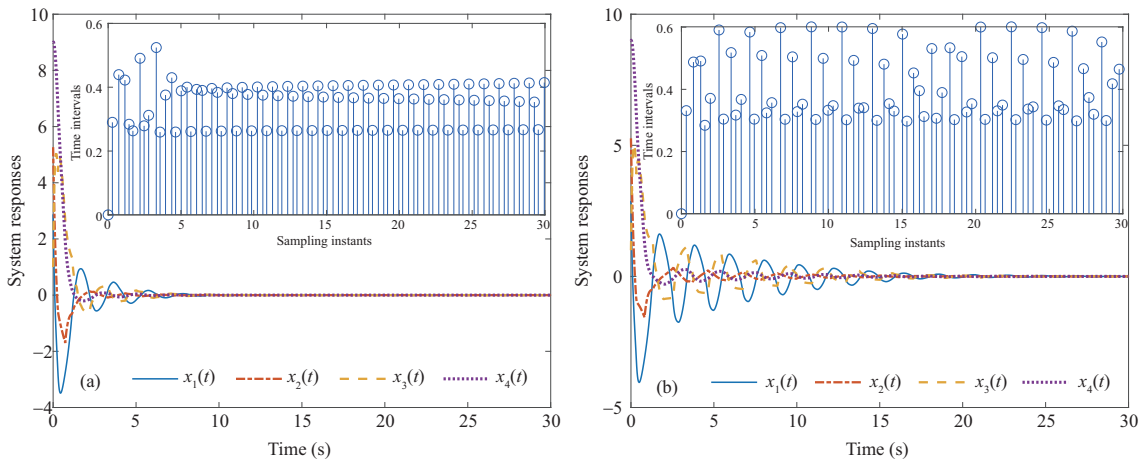

Figure 3 (Color online) State responses and time-intervals with (a) STS and (b) STS ($\eta = 1.2$).

period if compared with ETS1 and ETS2.

• The minimum inter-event time from ETS3 is also bigger than that from ETS1 and ETS2.

• From Figure 2(c), with ETS3, the closed-loop system reaches its steady states more slowly than ETS1 and ETS2. However, if reducing the threshold δ from 0.1 to 0.01, the system can quickly reach its steady states, which is shown in Figure 2(d) (ETS3 with $\delta = 0.01$ is called ETS3a for convenience). With ETS3a, the number of events triggered, the average period and the minimum inter-event time are also listed in Table 1, which are still competitive if compared with ETS1 and ETS2. Clearly, ETS3 also offers a trade-off between fewer events and faster convergence.

Next, we turn to the self-triggered implementation of the ETS3. Let $\delta = 0.1$, $\Omega = I$, $\beta_0 = 1$, $c_w = 0.01$ and $\eta = 1.05$. Then with the STS (39), the state responses of the closed-loop system (5) and the time intervals between two consecutive events are depicted in Figure 3(a). With the STS, the number of events triggered, the average period and the minimum inter-event time during $[0, 30]$ s are given in Table 1. It is clear to see from Figure 3(a) and Table 1 that the STS works pretty well. If we increase η to 1.2, the system reaches its steady state more slowly, which can be seen from Figure 3(b) while the number of events triggered is 73, less than that of STS with $\eta = 1.05$ (see Table 1).

Example 2. Consider an inverted pendulum on the top of a moving cart, where y is the cart's position and θ the pendulum bob's angle with respect to the vertical. Let $x = \mathrm{col}\{y, \dot{y}, \theta, \dot{\theta}\}$. Then its linearized state equation can be given by (4) with [23]

$$A = \begin{bmatrix} 0 & 1 & 0 & 0 \\ 0 & 0 & -10m/M & 0 \\ 0 & 0 & 0 & 1 \\ 0 & 0 & 10/l & 0 \end{bmatrix}, \quad B = \begin{bmatrix} 0 \\ 1/M \\ 0 \\ -1/(Ml) \end{bmatrix}, \quad D = \begin{bmatrix} 1 \\ 1 \\ 1 \\ 1 \end{bmatrix},$$

where m, M and l are the mass of the pendulum bob, the cart mass, and the length of the pendulum arm, respectively. Similar to [23], we set $m = 1$, $M = 10$ and $l = 3$, and assumed that $\|w(t)\| \leqslant 0.01\|x(t)\|$ [31].

Let $C = 0.3I$, $E = 0$ and $F = 0$. For the inverted pendulum system, the H_∞ control issue is investigated in [23], where a mixed pattern on sampling and transmission is devised. According to the mixed pattern, the system state is sampled periodically while whether the sampled data will be transmitted is determined by an event-triggering condition. Suppose that the gain K is given a priori as $K = K_1 = [2\ 12\ 378\ 210]$. Setting $\gamma = 200$, then employing Theorem 1 in [23], the admissible maximum sampling period that remains the system stability is 0.15 s, and it becomes smaller if one improves the performance index γ less than 200.

First, we show that the proposed ETS in this paper can deliver a better performance level γ for a larger allowable maximum $T_{\max}$. In fact, for a better performance index $\gamma = 60$, applying Proposition 1 with $\delta = 0.02$, the maximum value of $T_{\max}$ is obtained as 0.375 s, which is larger than 0.15 s

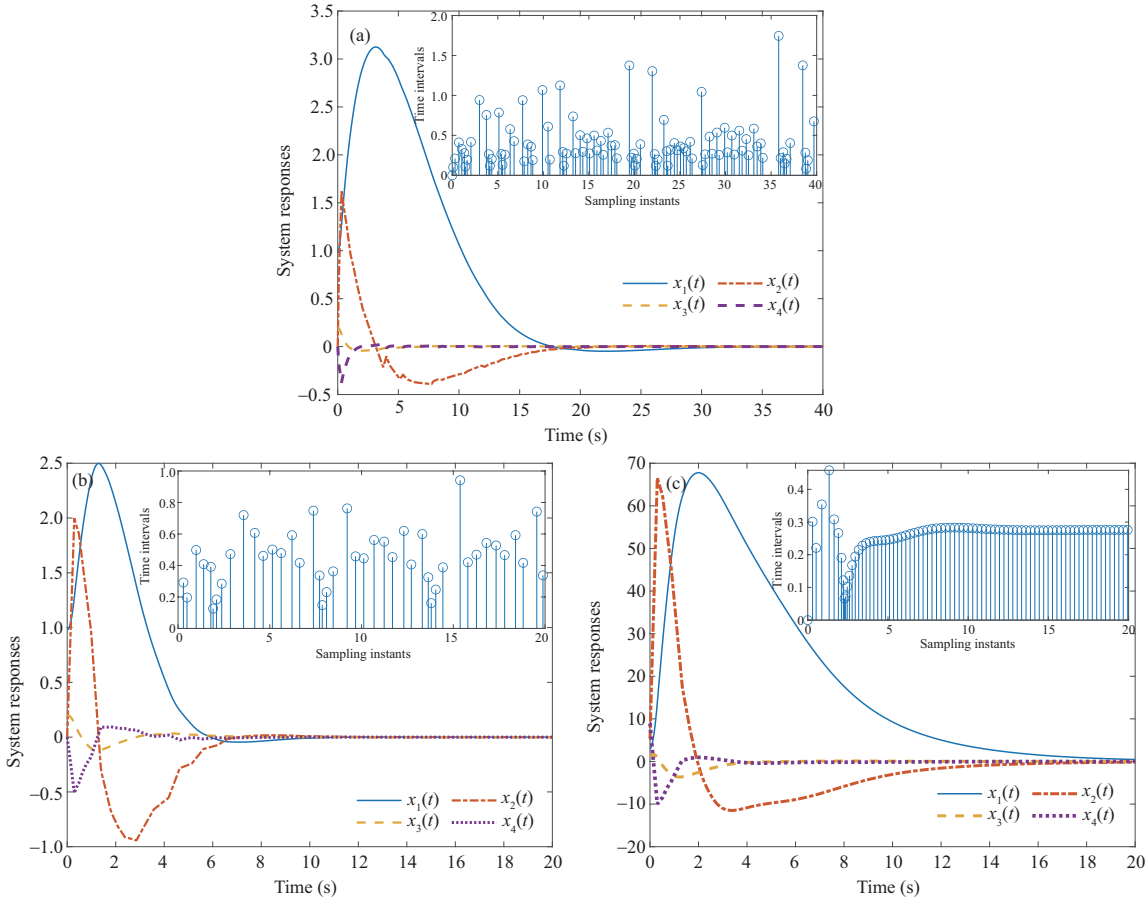

Figure 4 (Color online) State responses and time-intervals for Example 2 under (a) $u = K_1x$, (b) $u = K_2x$, and (c) $u = K_2x$ (self-triggered implementation).

in [23]. Specifically, for $T_{\max} = 0.35$ s, solving the linear matrix inequalities (25) and (26) gives Ω as

$$\Omega = \begin{bmatrix} 4.2805 & 28.046 & 122.46 & 659.99 \\ 28.046 & 184.98 & 1129.5 & 4325.7 \\ 122.46 & 1129.5 & 7583.8 & 26334 \\ 659.99 & 4325.7 & 26334 & 101891 \end{bmatrix}.$$

With the proposed event-triggered sampling scheme, Figure 4(a) depicts the sampling instants and the time intervals between two consecutive sampling instants; and the system states under the given controller are also shown in Figure 4(a), where the system initial state is given by $x_0 = \text{col}\{0.98, 0, 0.2, 0\}$. From Figure 4(a), during $[0, 40]$ s, just 97 events are triggered to sample the system state, and the average sampling period is 0.4093 s.

Next, we show that we can co-design both a suitable controller gain K and a weighting matrix Ω for a given threshold δ. For this goal, we set $\gamma = 20$, $\delta = 0.02$, $\epsilon_1 = 2$, $\epsilon_2 = 1$, applying Proposition 2, it is found that the linear matrix inequalities (33) and (34) are feasible for $T_{\max} = 0.492$ s, and the corresponding Ω and K are given by

$$\Omega = \begin{bmatrix} 3.3760 & 6.3517 & 122.97 & 68.91 \\ 6.3517 & 11.9543 & 231.41 & 129.68 \\ 122.97 & 231.41 & 4480.5 & 2510.7 \\ 68.91 & 129.68 & 2510.7 & 1406.9 \end{bmatrix},$$

$$K = K_2 = \begin{bmatrix} 6.5648 & 18.17 & 319.23 & 179.29 \end{bmatrix}.$$

From the calculations above, it is clear that under the designed ETS and controller, the closed-loop system can achieve a better performance level γ for a larger upper bound $T_{\max}$. Furthermore, with the designed ETS, Figure 4(b) depicts the sampling time instants and the time-intervals between two consecutive sampling instants. Within 20 s starting from zero, 45 events in all are triggered, leading to the average sampling period 0.4419 s. Under the designed control, Figure 4(b) also shows the state trajectories of the closed-loop system, from which it is clear that the designed controller works pretty well to ensure that the system is asymptotically stable.

Then, we turn to the self-triggered implementation of the designed ETS. Let $c_w = 0.01$, $\eta = 1.08$, $\beta_0 = 1$ and $T_{\max} = 0.492$. Then using the self-triggered strategy (39), the state trajectories of the closed-loop system with $u = K_2 x$ and the sampling instants are plotted in Figure 4(c). From this figure, during $[0, 20]$ s, there are 78 events triggered with the average sampling period 0.2556 s, which is smaller than 0.4419 s. Moreover, the state trajectories approach zero more slowly if compared with those in Figure 4(b).

5 Conclusion

The event-triggered H_∞ control of sampled-data control systems has been investigated. A novel ETS has been devised by comparing the integral of the state increment from t_k to t with the latest sampled state at t_k. It has been proven that the proposed ETS can avoid the Zeno behaviour. By employing the looped functional method, H_∞ performance analysis has been made and a corresponding criterion has been obtained to ensure a certain performance level of the closed-loop system. Based on the criterion, an LMI-based algorithm has been developed to co-design both the control gain and the weighting matrix in the ETS. Moreover, a self-triggered strategy has been presented to implement the proposed ETS. A batch reactor model and an inverted pendulum system have been finally given to validate the effectiveness of the proposed method.

Acknowledgements This work was partly supported by Key Project of Natural Science Foundation of Zhejiang Province of China (Grant No. LZ19F03000) and National Natural Science Foundation of China (Grant No. 62173209).

References

1 Fujioka H. Stability analysis of systems with aperiodic sample-and-hold devices. Automatica, 2009, 45: 771–775
2 Hetel L, Fiter C, Omran H, et al. Recent developments on the stability of systems with aperiodic sampling: an overview. Automatica, 2017, 76: 309–335
3 Hu Z, Ren H, Deng F, et al. Stabilization of sampled-data systems with noisy sampling intervals and packet dropouts via a discrete-time approach. IEEE Trans Autom Control, 2022, 67: 3204–3211
4 Tang G, Xue W, Fang H, et al. On the reinforcement learning extended state observer for a class of uncertain sampled-data control systems. Sci China Inf Sci, 2023, 66: 170205
5 Wang X H, Wang Z, Xia J W, et al. Adaptive event-trigger-based sampled-data stabilization of complex-valued neural networks: a real and complex LMI approach. Sci China Inf Sci, 2023, 66: 149203
6 Zeng H B, Teo K L, He Y. A new looped-functional for stability analysis of sampled-data systems. Automatica, 2017, 82: 328–331
7 Zhang D, Han Q L, Zhang X M. Network-based modeling and proportional-integral control for direct-drive-wheel systems in wireless network environments. IEEE Trans Cybern, 2020, 50: 2462–2474
8 Astrom K, Bernhardsson B. Comparison of periodic and event-based sampling for the first order stochastic systems. In: Proceedings of IFAC World Conference, 1999. 301–306
9 Zhang X M, Han Q L, Ge X, et al. Sampled-data control systems with non-uniform sampling: a survey of methods and trends. Annu Rev Control, 2023, 55: 70–91
10 Tabuada P. Event-triggered real-time scheduling of stabilizing control tasks. IEEE Trans Autom Control, 2007, 52: 1680–1685
11 Wang X, Sun J, Deng F, et al. Event-triggered consensus control of heterogeneous multi-agent systems: model- and data-based approaches. Sci China Inf Sci, 2023, 66: 192201
12 Xiao H C, Ding D R, Dong H L, et al. Adaptive event-triggered state estimation for large-scale systems subject to deception attacks. Sci China Inf Sci, 2022, 65: 122207
13 Sun Q, Chen J C, Shi Y. Event-triggered robust MPC of nonlinear cyber-physical systems against DoS attacks. Sci China Inf Sci, 2022, 65: 110202
14 Shi Y, Hu Q, Shao X, et al. Adaptive neural coordinated control for multiple Euler-Lagrange systems with periodic event-triggered sampling. IEEE Trans Neural Netw Learn Syst, 2023, 34: 8791–8801
15 Tang Y, Jin X, Shi Y, et al. Event-triggered attitude synchronization of multiple rigid body systems with velocity-free measurements. Automatica, 2022, 143: 110460
16 Yu H, Hao F. Input-to-state stability of integral-based event-triggered control for linear plants. Automatica, 2017, 85: 248–255
17 Li T F, Fu J, Deng F, et al. Stabilization of switched linear neutral systems: an event-triggered sampling control scheme. IEEE Trans Autom Control, 2018, 63: 3537–3544
18 Liu W, Ma Q, Xu S, et al. State quantized output feedback control for nonlinear systems via event-triggered sampling. IEEE Trans Autom Control, 2022, 67: 6810–6817

19 Peng C, Li F. A survey on recent advances in event-triggered communication and control. Inf Sci, 2018, 457-458: 113–125
20 Mousavi S H, Ghodrat M, Marquez H J. Integral-based event-triggered control scheme for a general class of non-linear systems. IET Control Theor Appl, 2015, 9: 1982–1988
21 Zhang L, Nguang S K, Ouyang D, et al. Synchronization of delayed neural networks via integral-based event-triggered scheme. IEEE Trans Neural Netw Learn Syst, 2020, 31: 5092–5102
22 Borgers D P, Heemels W P M H. Event-separation properties of event-triggered control systems. IEEE Trans Autom Control, 2014, 59: 2644–2656
23 Peng C, Han Q L. A novel event-triggered transmission scheme and $\mathcal{L}_2$ control co-design for sampled-data control systems. IEEE Trans Autom Control, 2013, 58: 2620–2626
24 Yue D, Tian E, Han Q L. A delay system method for designing event-triggered controllers of networked control systems. IEEE Trans Autom Control, 2013, 58: 475–481
25 Zhang X M, Han Q L. A decentralized event-triggered dissipative control scheme for systems with multiple sensors to sample the system outputs. IEEE Trans Cybern, 2016, 46: 2745–2757
26 Miskowicz M. Asymptotic effectiveness of the event-based sampling according to the integral criterion. Sensors, 2007, 7: 16–37
27 Seuret A. A novel stability analysis of linear systems under asynchronous samplings. Automatica, 2012, 48: 177–182
28 Wu M, He Y, She J H. New delay-dependent stability criteria and stabilizing method for neutral systems. IEEE Trans Autom Control, 2004, 49: 2266–2271
29 Walsh G, Ye H. Scheduling of networked control systems. IEEE Control Sys Mag, 2001, 21: 57–65
30 Mazo M, Anta A, Tabuada P. On self-triggered control for linear systems: guarantees and complexity. In: Proceedings of the 10th European Control Conference, 2009. 3767–3772
31 Wang X F, Lemmon M D. Self-triggered feedback control systems with finite-gain $\mathcal{L}_2$ stability. IEEE Trans Autom Control, 2009, 54: 452–467
32 Zhang X M, Han Q L, Zeng Z. Hierarchical type stability criteria for delayed neural networks via canonical bessel-legendre inequalities. IEEE Trans Cybern, 2018, 48: 1660–1671

Appendix A Proof of Proposition 1

To begin with, we introduce Lemma 1.

Lemma 1 ([32]). For an $n\times n$ real positive definite matrix R, and a p-dimensional vector ξ satisfying $\mathrm{col}\{x(b), x(a), \frac{1}{b-a}\int_a^b x(s)\mathrm{d}s\} = \mathscr{C}\xi$ with $\mathscr{C}$ being a real matrix, the following inequality holds for any matrix $\mathcal{M}\in\mathbb{R}^{2n\times p}$:

$$-\int_a^b \dot{x}^{\mathrm{T}}(s)R\dot{x}(s)\mathrm{d}s \leqslant \xi^{\mathrm{T}}\mathscr{F}_a^b(\mathscr{C}, R, \mathcal{M})\xi, \tag{A1}$$

where

$$\begin{aligned}&\mathscr{F}_a^b(\mathscr{C}, R, \mathcal{M}) := \mathscr{C}^{\mathrm{T}}\Theta^{\mathrm{T}}\mathcal{M} + \mathcal{M}^{\mathrm{T}}\Theta\mathscr{C} + (b-a)\mathcal{M}^{\mathrm{T}}\mathcal{R}^{-1}\mathcal{M},\\ &\Theta := \begin{bmatrix} I & -I & 0\\ I & I & -2I\end{bmatrix},\quad \mathcal{R} := \mathrm{diag}\{R, 3R\}.\end{aligned}$$

Now, we start to prove the conclusion. Introduce a vector as

$$\begin{aligned}&\xi(t) = \mathrm{col}\{\dot{x}(t), x(t), x(t_k), x(t_{k+1}), \upsilon_1(t), \upsilon_2(t), \upsilon_3(t), \upsilon_4(t)\},\\ &\upsilon_3(t) = \frac{1}{t-t_k}\int_{t_k}^t x(s)\mathrm{d}s,\ \ \upsilon_4(t) = \frac{1}{t_{k+1}-t}\int_t^{t_{k+1}} x(s)\mathrm{d}s.\end{aligned}$$

Then taking the time derivative yields

$$\dot{\mathcal{W}}(t) = 2x^{\mathrm{T}}(t)P\dot{x}(t) + \dot{\mathcal{V}}_0(t), \tag{A2}$$

where

$$\begin{aligned}\dot{\mathcal{V}}_0(t) =\ & 2\xi^{\mathrm{T}}(t)(C_1^{\mathrm{T}}Q_1C_2 + C_3^{\mathrm{T}}Q_1C_4 + C_{51}^{\mathrm{T}}Q_2C_{61} - C_{52}^{\mathrm{T}}Q_2C_{62})\xi(t)\\ &+ (t_{k+1}-t)\xi^{\mathrm{T}}(t)(C_7^{\mathrm{T}}Q_3C_7 + e_1^{\mathrm{T}}R_1e_1)\xi(t) + (t-t_k)\xi^{\mathrm{T}}(t)(e_1^{\mathrm{T}}R_2e_1 - C_7^{\mathrm{T}}Q_3C_7)\xi(t)\\ &- \int_{t_k}^t \dot{x}^{\mathrm{T}}(s)R_1\dot{x}(s)\mathrm{d}s - \int_t^{t_{k+1}} \dot{x}^{\mathrm{T}}(s)R_2\dot{x}(s)\mathrm{d}s,\end{aligned} \tag{A3}$$

$C_2 = C_{20} + (t-t_k)C_{21} + (t_{k+1}-t)C_{22}$, and $C_4 = (t-t_k)C_{41} + (t_{k+1}-t)C_{42}$. Note that $\mathrm{col}\{x(t), x(t_k), \upsilon_3(t)\} = \mathscr{C}_1\xi(t)$ and $\mathrm{col}\{x(t_{k+1}), x(t), \upsilon_4(t)\} = \mathscr{C}_2\xi(t)$. By Lemma 1, one has, for compatible real matrices $\mathcal{M}_i$

$$\begin{aligned}&-\int_{t_k}^t \dot{x}^{\mathrm{T}}(s)R_1\dot{x}(s)\mathrm{d}s \leqslant \xi^{\mathrm{T}}(t)\mathscr{F}_{t_k}^t(\mathscr{C}_1, R_1, \mathcal{M}_1)\xi(t),\\ &-\int_t^{t_{k+1}} \dot{x}^{\mathrm{T}}(s)R_2\dot{x}(s)\mathrm{d}s \leqslant \xi^{\mathrm{T}}(t)\mathscr{F}_t^{t_{k+1}}(\mathscr{C}_2, R_2, \mathcal{M}_2)\xi(t),\end{aligned}$$

where $\mathscr{F}_a^b(\cdot,\cdot,\cdot)$ is defined in Lemma 1. Let $T_k = t_{k+1} - t_k$. Then

$$\dot{\mathcal{W}}(t) \leqslant \xi^{\mathrm{T}}(t)\left[\frac{(t_{k+1}-t)\,\Psi_1 + (t-t_k)\,\Psi_2}{T_k}\right]\xi(t), \tag{A4}$$

where $\Psi_1 := \Phi_1 + T_k(\Gamma_1 + \mathcal{M}_2^{\mathrm{T}}\mathcal{R}_2^{-1}\mathcal{M}_2)$, $\Psi_2 := \Phi_1 + T_k(\Gamma_2 + \mathcal{M}_1^{\mathrm{T}}\mathcal{R}_1^{-1}\mathcal{M}_1)$ with Φ_1, Γ_1 and Γ_2 being defined in (29), (31) and (32), respectively. Under the ETS (18), for $t \in [t_k, t_{k+1})$, we have (22). On the other hand, it is clear that $\upsilon_1(t) = (t-t_k)[\upsilon_3(t) - x(t_k)]$ and $\upsilon_2(t) = (t_{k+1} - t)\upsilon_4(t)$. Thus, for three matrices N_1, N_2 and N_3, the following hold:

$$2\xi^{\mathrm{T}}(t)N_1^{\mathrm{T}}\{\upsilon_1(t) - (t-t_k)[\upsilon_3(t) - x(t_k)]\} = 0, \tag{A5}$$

$$2\xi^{\mathrm{T}}(t)N_2^{\mathrm{T}}[\upsilon_2(t) - (t_{k+1} - t)\upsilon_4(t)] = 0, \tag{A6}$$

$$2\xi^{\mathrm{T}}(t)N_3^{\mathrm{T}}[-\dot{x}(t) + Ax(t) + BKx(t_k) + Dw(t)] = 0. \tag{A7}$$

From (22), and (A5)–(A7), it is easy to get

$$0 \leqslant \xi^{\mathrm{T}}(t)\left[\frac{(t_{k+1}-t)\,\Psi_3 + (t-t_k)\,\Psi_4}{T_k}\right]\xi(t) + 2\xi^{\mathrm{T}}(t)N_3^{\mathrm{T}}Dw(t),$$

where $\Psi_3 = \Phi_2 + T_k\mathrm{He}\{-N_2^{\mathrm{T}}e_8\}$ and $\Psi_4 = \Phi_2 + T_k\mathrm{He}\{N_1^{\mathrm{T}}(e_3 - e_7)\}$ with Φ_2 given in (30). To sum up, we have that

$$\dot{\mathcal{W}}(t) \leqslant \xi^{\mathrm{T}}(t)\left[\frac{(t_{k+1}-t)\Upsilon_1 + (t-t_k)\Upsilon_2}{T_k}\right]\xi(t) + 2\xi^{\mathrm{T}}(t)N_3^{\mathrm{T}}Dw(t), \tag{A8}$$

where $\Upsilon_1 = \Phi_1 + \Phi_2 + T_k\big(\Gamma_1 - \mathrm{He}\{N_2^{\mathrm{T}}e_8\} + \mathcal{M}_2^{\mathrm{T}}\mathcal{R}_2^{-1}\mathcal{M}_2\big)$ and $\Upsilon_2 = \Phi_1 + \Phi_2 + T_k\big(\Gamma_2 + \mathrm{He}\{N_1^{\mathrm{T}}(e_3 - e_7)\} + \mathcal{M}_1^{\mathrm{T}}\mathcal{R}_1^{-1}\mathcal{M}_1\big)$.

We now prove the conclusion from two aspects. First, for $w(t) \equiv 0$, one has

$$\dot{\mathcal{W}}(t) \leqslant \xi^{\mathrm{T}}(t)\left[\frac{(t_{k+1}-t)\Upsilon_1 + (t-t_k)\Upsilon_2}{T_k}\right]\xi(t). \tag{A9}$$

If the linear matrix inequalities (25) and (26) are satisfied, then $\Upsilon_1 < 0$ and $\Upsilon_2 < 0$, leading to $\dot{\mathcal{W}}(t) < 0$. By employing [27, Theorem 1], one can conclude that the system is asymptotically stable.

Next, for $w(t) \neq 0$, let $L_0 = Ce_2 + EKe_3$. Then

$$\begin{aligned} z^{\mathrm{T}}(t)z(t) - \gamma^2 w^{\mathrm{T}}(t)w(t) + \dot{\mathcal{W}}(t) \leqslant & \begin{bmatrix}\xi(t)\\ w(t)\end{bmatrix}^{\mathrm{T}}\left\{\frac{t_{k+1}-t}{T_k}\left(\begin{bmatrix}\Upsilon_1 & N_3^{\mathrm{T}}D\\ \star & -\gamma^2 I\end{bmatrix} + \begin{bmatrix}L_0^{\mathrm{T}}\\ F^{\mathrm{T}}\end{bmatrix}[L_0\ F]\right)\right.\\ & \left. + \frac{t-t_k}{T_k}\left(\begin{bmatrix}\Upsilon_2 & N_3^{\mathrm{T}}D\\ \star & -\gamma^2 I\end{bmatrix} + \begin{bmatrix}L_0^{\mathrm{T}}\\ F^{\mathrm{T}}\end{bmatrix}[L_0\ F]\right)\right\}\begin{bmatrix}\xi(t)\\ w(t)\end{bmatrix}. \end{aligned}$$

Thus, $z^{\mathrm{T}}(t)z(t) - \gamma^2 w^{\mathrm{T}}(t)w(t) + \dot{\mathcal{W}}(t) \leqslant 0$ if the following matrix inequalities are feasible:

$$\begin{bmatrix}\Upsilon_1 & N_3^{\mathrm{T}}D & L_0^{\mathrm{T}}\\ \star & -\gamma^2 I & F^{\mathrm{T}}\\ \star & \star & -I\end{bmatrix} < 0, \quad \begin{bmatrix}\Upsilon_2 & N_3^{\mathrm{T}}D & L_0^{\mathrm{T}}\\ \star & -\gamma^2 I & F^{\mathrm{T}}\\ \star & \star & -I\end{bmatrix} < 0, \tag{A10}$$

which are ensured by (25) and (26). Integrating from t_k to t_{k+1}, and after some simple calculation, we can obtain $J < 0$ under zero initial conditions.

Appendix B Proof of Proposition 2

We complete the proof based on Proposition 1. In doing so, let $\tilde{\epsilon}_0 = e_1 + \epsilon_1 e_2 + \epsilon_2 e_3$ and $N_3 = N\tilde{\epsilon}_0$, where ϵ_1 and ϵ_2 are two constants, and N is a real matrix. If the matrix inequalities (25) and (26) are satisfied, then N is convertible holds due to

$$e_1\big\{\Phi_1 + \Phi_2 + T_k[\Gamma_1 - \mathrm{He}\{N_2^{\mathrm{T}}e_8\}]\big\}e_1^{\mathrm{T}} = -N - N^{\mathrm{T}} + R_1 < 0.$$

Next, we are to design the control gain K. Let

$$\begin{aligned} &\mathcal{T}_1 = e_1^{\mathrm{T}}N^{-1}e_1 + e_2^{\mathrm{T}}N^{-1}e_2 + \cdots + e_8^{\mathrm{T}}N^{-1}e_8,\\ &\mathcal{T}_2 = \mathrm{diag}\{N^{-1}, N^{-1}\},\ \mathcal{T} = \mathrm{diag}\{\mathcal{T}_1, I, I, \mathcal{T}_2\}, \end{aligned} \tag{B1}$$

and $X = N^{-1}$, $\bar{P} = X^{\mathrm{T}}PX$, $\bar{R}_1 = X^{\mathrm{T}}R_1$, $\bar{R}_2 = X^{\mathrm{T}}R_2X$,

$$\begin{aligned} &\bar{Q}_1 = \mathrm{diag}\{X^{\mathrm{T}}, X^{\mathrm{T}}, X^{\mathrm{T}}, X^{\mathrm{T}}, X^{\mathrm{T}}\}Q_1\mathrm{diag}\{X, X, X, X\},\\ &\bar{Q}_j = \mathrm{diag}\{X^{\mathrm{T}}, X^{\mathrm{T}}\}Q_j\mathrm{diag}\{X, X\},\ j = 2, 3,\ \bar{\Omega} = X^{\mathrm{T}}\Omega X,\\ &\bar{N}_i = X^{\mathrm{T}}N_iX,\quad \tilde{\mathcal{M}}_i = \mathcal{T}_1^{\mathrm{T}}\mathcal{M}_i^{\mathrm{T}}\mathcal{T}_2,\ i = 1, 2,\ Y = KX. \end{aligned}$$

Then

$$\mathcal{T}^{\mathrm{T}}\beth_1\mathcal{T} = \begin{bmatrix}\mathcal{T}_1^{\mathrm{T}}\beth_{11}\mathcal{T}_1 & \mathcal{T}_1^{\mathrm{T}}\tilde{\epsilon}_0^{\mathrm{T}}N^{\mathrm{T}}D & \mathcal{T}_1^{\mathrm{T}}L_0^{\mathrm{T}} & T_k\mathcal{T}_1^{\mathrm{T}}\mathcal{M}_2^{\mathrm{T}}\mathcal{T}_2\\ \star & -\gamma^2 I & F^{\mathrm{T}} & 0\\ \star & \star & -I & 0\\ \star & \star & \star & -T_k\mathcal{T}_2^{\mathrm{T}}\mathcal{R}_2\mathcal{T}_2\end{bmatrix},$$

$$\mathcal{T}^{\mathrm{T}}\beth_2\mathcal{T} = \begin{bmatrix}\mathcal{T}_1^{\mathrm{T}}\beth_{21}\mathcal{T}_1 & \mathcal{T}_1^{\mathrm{T}}\tilde{\epsilon}_0^{\mathrm{T}}N^{\mathrm{T}}D & \mathcal{T}_1^{\mathrm{T}}L_0^{\mathrm{T}} & T_k\mathcal{T}_1^{\mathrm{T}}\mathcal{M}_1^{\mathrm{T}}\mathcal{T}_2\\ \star & -\gamma^2 I & F^{\mathrm{T}} & 0\\ \star & \star & -I & 0\\ \star & \star & \star & -T_k\mathcal{T}_2^{\mathrm{T}}\mathcal{R}_1\mathcal{T}_2\end{bmatrix}.$$

It is clear that $\mathcal{T}^{\mathrm{T}}\beth_1\mathcal{T} < 0$ and $\mathcal{T}^{\mathrm{T}}\beth_2\mathcal{T} < 0$ are equivalent to (33) and (34), respectively. Moreover, a solution to (K, Ω) can be given as $(K, \Omega) = (YX^{-1}, X^{-\mathrm{T}}\bar{\Omega}X^{-1})$.